

Far-ultraviolet photolysis of solid methane

Jen-Iu Lo,¹ Meng-Yeh Lin,¹ Yu-Chain Peng,¹ Sheng-Lung Chou,¹ Hsiao-Chi Lu,¹
Bing-Ming Cheng^{1*} and J. F. Ogilvie²

¹National Synchrotron Radiation Research Center, 101 Hsin-Ann Road, Hsinchu Science Park, Hsinchu 30076, Taiwan

²Escuela de Química y CELEQ, Universidad de Costa Rica, Ciudad Universitaria Rodrigo Facio, San Pedro de Montes de Oca, San Jose 11501–2060, Costa Rica

Accepted 2015 April 23. Received 2015 April 22; in original form 2015 March 03

ABSTRACT

Irradiation of samples of pure solid methane at 3 K with far-ultraviolet light from a synchrotron yielded products CH₃, C₂H₂, C₂H₄ and C₂H₆ that were quantitatively identified through their infrared absorption spectra. The greatest wavelengths at which products CH₃, C₂H₄, C₂H₆ and C₂H₂ were generated were 140, 140, 175 and 190 nm, respectively. *Cassini* spacecraft has observed the condensed methane on Titan. The observation demonstrates the existence of pure condensed methane in astro-environments. Information about the dissociation of CH₄ at a low temperature with photons of varied energy has implications for astrophysical environments.

Key words: astrochemistry – molecular processes – methods: laboratory: atomic – ISM: molecules – infrared: ISM.

1 INTRODUCTION

The hydrocarbon most abundant in space is methane, followed by C₂H₆, C₂H₂ and C₂H₄, which are believed to be produced from methane induced by photons, electrons and other energetic particles (Yung & DeMore 1999). Methane is the simplest non-radical hydrocarbon in space, has been proposed as a precursor in the synthesis of complicated organic molecules and is believed to play a key role in the formation of prebiotic molecules (Markwick et al. 2000). The photochemistry of methane in the gaseous phase has been thus extensively investigated (Wang & Liu 1998; Cook et al. 2001; Romanzin et al. 2005; Gans et al. 2011). In cold outer space, methane exists in condensed phases; for example, at the temperatures of Pluto, Triton and other trans-Neptunian objects that are typically less than 40 K, methane occurs there in a solid form (Quirico et al. 1999; Olkin et al. 2007; Tegler et al. 2010). At the *Infrared Space Observatory*, infrared spectra of solid methane were recorded from ~30 protostars (White et al. 2000; Gürtler et al. 2002; Alexander et al. 2003), the galactic centre (Chiar et al. 2000) and an external galactic nucleus (Spoon et al. 2001). The chemistry of methane in a condensed phase might differ appreciably from that of gaseous methane; varied sources of radiation to destroy CH₄ molecules might produce varied daughter species in space. Because far-ultraviolet radiation is one driving force to dissociate methane in astronomical environments, the photochemistry of methane in condensed phases warrants attention.

The photon flux of solar radiation from 400 to 700 nm is 10³–10⁶ times that from 200 to 100 nm (Rottman 1981; Mount & Rottman

1983); the latter range includes mostly emission lines, such as H Lyman- α at 121.6 nm, superimposed on a continuum rapidly decreasing with decreasing wavelength. The energy of photons at 121.6 nm, much greater than that for visible light, is enough to break almost any chemical bond in any molecule. Light of wavelength less than 200 nm is hence likely to be an important driving force to generate chemical compounds in not only our Solar system but also other spatial environments. The interaction of galactic cosmic rays with interstellar molecules generates secondary fields of vacuum-ultraviolet (VUV) radiation, the so-called *cosmic-ray-induced photons* (Cecchi-Pestellini & Aiello 1992); this radiation can subsequently induce the photolysis of molecules in interstellar clouds or those in other astrophysical environments.

Kaiser & Roessler (1998) irradiated solid methane with 9.0 MeV α -particles and with 7.3 MeV protons; the major products were C₂H₂, C₂H₄ and C₂H₆. Baratta et al. (2003) exposed pure solid methane ice to argon ions of energy 60 keV, and identified species C₂H₂, C₂H₄, C₂H₆ and C₃H₈ from infrared absorption spectra. Bennett et al. (2006) bombarded solid methane with energetic electrons and focused on the identification of species CH_x ($x = 1$ –4) and C₂H_x ($x = 2$ –6). de Barros et al. (2011) bombarded a layer of methane ice with oxygen ions of energy 220 MeV, and detected species including CH₃, C₂H₂, C₂H₄, C₂H₆ and C₃H₈ according to their infrared spectra. Using a lamp based on a microwave discharge of flowing hydrogen, Gerakines, Schutte and Ehrenfreund (1996) conducted experiments with UV photolysis of pure solid CH₄ at 10 K; they observed products CH₃, C₂H₄, C₂H₆, C₃H₄, C₃H₈ and other unidentified species.

Photons in far-ultraviolet light and energetic particles incident on molecular solids analogously induce varied effects in astrophysical environments. The photolysis of CH₄ with far-ultraviolet light

* E-mail: bmcheng@nsrrc.org.tw

undoubtedly serves as an initial process in the evolution of hydrocarbons in space. Our present investigation concerned the products of photolysis of solid methane at 3 K using far-ultraviolet light from a synchrotron. The photochemistry of methane in this solid phase differs from that of gaseous methane, which has implications for astrophysical environments.

2 EXPERIMENTS

The apparatus for photolysis of solid samples is similar to that described previously (Wu et al. 2008, 2010, 2012; Lin et al. 2014). Gaseous methane was deposited on a KBr window before photolysis with radiation at a selected wavelength; a closed-cycle refrigerator system (Janis RDK-415) cooled the KBr substrate to 3 K. A turbomolecular pump backed by a scroll pump evacuated the chamber to a pressure less than $4 \mu\text{Pa}$. The source of far-UV radiation was an undulator with periodically spaced permanent magnets (90 mm, U90) attached to the storage ring of an electron accelerator (energy 1.5 GeV) at National Synchrotron Radiation Research Center (NSRRC) in Taiwan. Harmonics from the undulator were suppressed through absorption by Ar at pressure 1.33 kPa and a filter – crystalline LiF for 121.6 nm, CaF_2 for 130, 140 and 155 nm, silica (Suprasil) for 165 and 175 nm, and quartz for 185, 190 and 200 nm.

At the selected wavelength, the samples of solid methane were photolyzed for periods 10 s, 30 s, 1 min, 5 min, 10 min, 30 min and another 30 min sequentially; the total duration of irradiation was 76 min and 40 s. The photon doses of each irradiation period were measured with a gold mesh (95 per cent transmission). IR absorption spectra were recorded at various stages of experiments with an interferometric infrared spectrometer (Bomem, DA8) equipped with a KBr beamsplitter and a HgCdTe detector (cooled to 77 K) to cover the spectral range $500\text{--}4000 \text{ cm}^{-1}$; 400–600 scans at resolution $0.2\text{--}0.5 \text{ cm}^{-1}$ were made at each stage of the experiment.

CH_4 (99.999 per cent, Matheson Gases), CD_4 (isotopic purity 99 per cent, Cambridge Isotopic Laboratory), $^{13}\text{CH}_4$ (isotopic purity 99.9 per cent, Cambridge Isotopic Laboratory), C_2H_2 (99.0 per cent, Matheson Gases), C_2H_4 (99.99 per cent, Matheson Gases) and C_2H_6 (99.995 per cent, Matheson Gases) were used without further purification.

3 RESULTS AND DISCUSSION

3.1 Infrared absorption of solid isotopic methanes

Fig. 1 presents infrared absorption spectra of isotopic solid methanes at 3 K. For comparison, the spectrum of a gaseous sample of $^{12}\text{CH}_4$ shows vibrational–rotational bands with centres near 1306.4 cm^{-1} , assigned to fundamental angular deformational mode ν_4 , and near 3018.9 cm^{-1} , associated with stretching mode ν_3 . Fig. 1(a) shows that the corresponding feature for ν_3 of pure solid $^{12}\text{CH}_4$ is amalgamated into one prominent line with maximum absorption at 3008.9 cm^{-1} and width 5.9 cm^{-1} , and a shoulder about 3021.2 cm^{-1} ; the feature for ν_4 of pure solid $^{12}\text{CH}_4$ that possesses a total width about 8.2 cm^{-1} exhibits a partially resolved doublet at 1301.5 and 1296.8 cm^{-1} with a shoulder at 1294.5 cm^{-1} , as shown in the inset. For pure solid $^{13}\text{CH}_4$ at 3 K, the feature in Fig. 1(b) for ν_3 shifts to 2998.8 cm^{-1} with a shoulder about 3010.8 cm^{-1} , whereas the ν_4 mode comprises a doublet at 1293.0 and 1288.9 cm^{-1} with a shoulder at 1286.3 cm^{-1} . For pure solid $^{12}\text{CD}_4$ at 3 K, the absorption in Fig. 1(c) associated with mode ν_3 comprises a single line at 2252.0 cm^{-1} ; the ν_4 mode shows a multiplex with maximum intensity at 990.6 cm^{-1} .

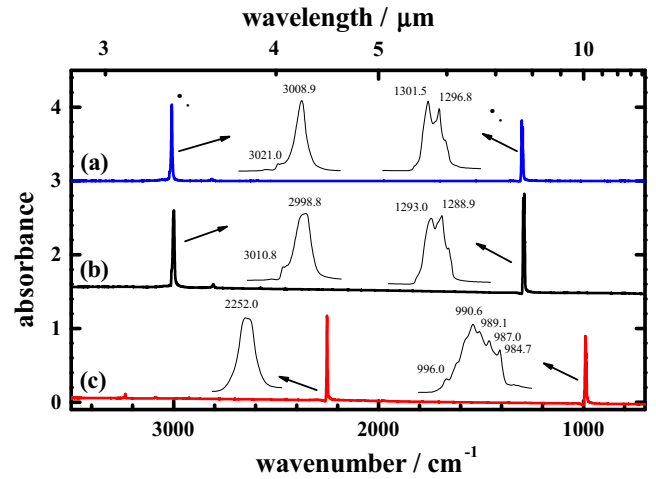


Figure 1. Absorption spectra of pure (a) $^{12}\text{CH}_4$ (ordinate scale offset +3.0), (b) $^{13}\text{CH}_4$ (ordinate scale offset +1.5), (c) and $^{12}\text{CD}_4$, all at 3 K; resolution 0.5 cm^{-1} from 600 co-added interferograms.

Features in IR absorption spectra of methane vary with the physical conditions of the sample. For example, the lines associated with mode ν_4 of $^{12}\text{CH}_4$ dispersed in solid neon with molar ratio 1000 at 3 K (Ogilvie et al. 2011) are fitted with 38 components, some having widths as small as 0.05 cm^{-1} , in the range $1311\text{--}1305 \text{ cm}^{-1}$; whereas the corresponding lines of $^{12}\text{CH}_4$ in pure solid methane show a partially resolved doublet with a total width about 8.2 cm^{-1} . As methane molecules dispersed in neon at molar ratio 1:1000 are effectively separated from one another, the absorption spectra of pure solid methane show the effects of interacting molecules.

3.2 Spectra of $\text{C}_2\text{H}_2/\text{CH}_4 = 1/250$, $\text{C}_2\text{H}_4/\text{CH}_4 = 1/250$ and $\text{C}_2\text{H}_6/\text{CH}_4 = 1/250$

According to previous work on irradiated solid methane, the major products generated are stable products C_2H_2 , C_2H_4 and C_2H_6 (Gerakines et al. 1996; Kaiser & Roessler 1998; Baratta et al. 2003; Bennett et al. 2006; de Barros et al. 2011). The wavenumbers of these species in solid methane might shift slightly from the corresponding wavenumbers of lines of the same molecules in a pure solid state or in the gaseous phase, which would perturb their identification in solid methane. To verify these shifts, we recorded separately the infrared spectra of solid $^{12}\text{CH}_4$ samples at 3 K containing $^{12}\text{C}_2\text{H}_2$ or $^{12}\text{C}_2\text{H}_4$ or $^{12}\text{C}_2\text{H}_6$ in trace proportion, 1/250, displayed in Fig. 2; the characteristic lines recorded and their assignments are listed in Table 1.

From our separate experiments with $^{12}\text{C}_2\text{H}_2:^{12}\text{CH}_4 = 1:250$, $^{12}\text{C}_2\text{H}_4:^{12}\text{CH}_4 = 1:250$ and $^{12}\text{C}_2\text{H}_6:^{12}\text{CH}_4 = 1:250$, we derived the ratios of absorption of $^{12}\text{C}_2\text{H}_2$, $^{12}\text{C}_2\text{H}_4$ and $^{12}\text{C}_2\text{H}_6$ dispersed in solid $^{12}\text{CH}_4$. According to Fig. 2, the vibrational modes of greatest absorbance are ν_5 of $^{12}\text{C}_2\text{H}_2$ at 736.6 cm^{-1} , ν_7 of $^{12}\text{C}_2\text{H}_4$ at 949.7 cm^{-1} and ν_{10} of $^{12}\text{C}_2\text{H}_6$ at 2975.7 cm^{-1} . When we integrated the intensities of these lines to compare the normalized values, we derived the ratios of their absorptions, as listed in Table 2; these normalized values allow us to generate absolute yields relative to that of C_2H_2 , which we employed in our analysis. Among these lines, mode ν_5 of $^{12}\text{C}_2\text{H}_2$ at 736.6 cm^{-1} possesses the greatest absorption coefficient; the ratios of mode ν_7 of $^{12}\text{C}_2\text{H}_4$ at 949.7 cm^{-1} and mode ν_{10} of $^{12}\text{C}_2\text{H}_6$ at 2975.7 cm^{-1} are 56.2 and 72.5 per cent, respectively. We calculated the A-factors of vibrational modes (Jamieson

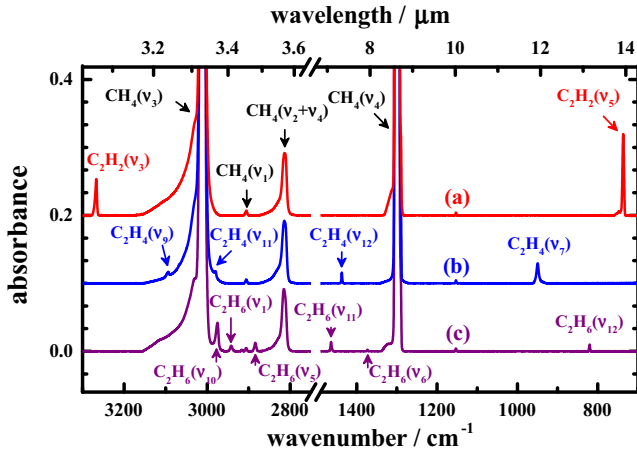


Figure 2. Absorption spectra of (a) $^{12}\text{C}_2\text{H}_2/^{12}\text{CH}_4 = 1/250$ (ordinate scale offset +0.2), (b) $^{12}\text{C}_2\text{H}_4/^{12}\text{CH}_4 = 1/250$ (ordinate scale offset +0.1), (c) $^{12}\text{C}_2\text{H}_6/^{12}\text{CH}_4 = 1/250$, all samples at 3 K; resolution 0.5 cm^{-1} from 600 co-added interferograms.

Table 1. Characteristic wavenumbers and assignments of vibrational modes of lines of $^{12}\text{C}_2\text{H}_6$, $^{12}\text{C}_2\text{H}_4$ and $^{12}\text{C}_2\text{H}_2$ at molar ratio 1/250 in solid $^{12}\text{CH}_4$ at 3 K.

Species	Wavenumber/ cm^{-1}
$^{12}\text{CH}_4$	1296.5 (ν_4), 2589.7 ($2\nu_4$), 2811.6 ($\nu_2+\nu_4$), 2905.7 (ν_1), 3009.7 (ν_3), 4201.1 ($\nu_1+\nu_4$), 4300.1 ($\nu_3+\nu_4$), 4528.4 ($\nu_2+\nu_3$)
$^{12}\text{C}_2\text{H}_2$	736.6 (ν_5), 3267.0 (ν_3)
$^{12}\text{C}_2\text{H}_4$	949.7 (ν_7), 1437.3 (ν_{12}), 2979.4 (ν_{11}), 3093.9 (ν_9)
$^{12}\text{C}_2\text{H}_6$	820.2 (ν_{12}), 1373.3 (ν_6), 1463.9 (ν_{11}), 2883.9 (ν_5), 2916.5 ($2\nu_8$), 2942.0 (ν_1), 2975.7 (ν_{10})

et al. 2005) at the B3LYP/aug-cc-pVTZ level of density-functional theory (Frisch et al. 2009) to obtain 196 km mol^{-1} for the A-factor of mode ν_5 of $^{12}\text{C}_2\text{H}_2$, 97.1 km mol^{-1} for mode ν_7 of $^{12}\text{C}_2\text{H}_4$ and 129 km mol^{-1} for mode ν_{10} of $^{12}\text{C}_2\text{H}_6$. Dobbs & Dixon (1994) calculated the A-factor of mode ν_7 of $^{12}\text{C}_2\text{H}_4$ as 96.7 km mol^{-1} , consistent with our value. According to these calculated A-factors of mode ν_5 of $^{12}\text{C}_2\text{H}_2$, the ratios of mode ν_7 of $^{12}\text{C}_2\text{H}_4$ and mode ν_{10} of $^{12}\text{C}_2\text{H}_6$ are 49.5 and 65.7 per cent, respectively. The discrepancies between calculated and experimental values of ratios are less than 10 per cent.

3.3 Absorption spectra of products from solid isotopic methanes at 3 K after photolysis at 121.6 nm

On irradiation of a sample of solid methane at 3 K with light of wavelength 121.6 nm, the intensity of all infrared absorption lines of precursor methane at 3 K uniformly decreased for the first 2 min, continuously, but at a rate decreasing with increasing duration of

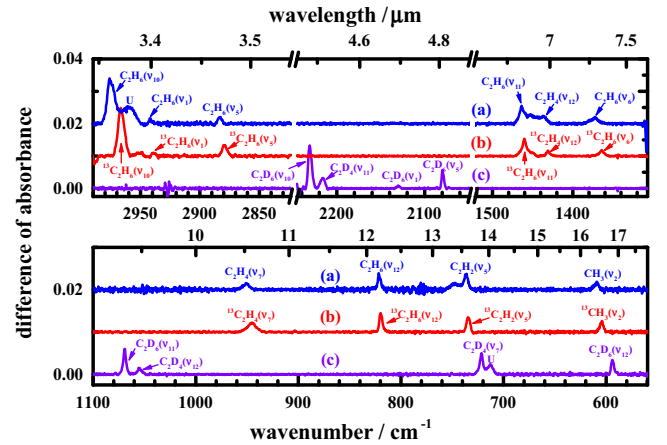


Figure 3. Difference spectra of solid methane at 3 K after irradiation at 121.6 nm for 76 min (a) $^{12}\text{CH}_4$ (ordinate scale offset +0.02); (b) $^{13}\text{CH}_4$ (ordinate scale offset +0.01); (c) $^{12}\text{CD}_4$; resolution 0.5 cm^{-1} , from 600 co-added interferograms.

irradiation. After irradiation for 76 min total as an accumulation of several smaller periods and as limited by the total available duration of experiments, the intensities of lines of CH_4 decreased by ~ 24 per cent; the extent of depletion was derived from a comparison of the ratios of net absorbance at a particular duration with those of the original sample.

Through their characteristic infrared absorption lines, our experiments with methane containing ^{12}C , ^{13}C , H and D enabled a definitive identification of photolysis products, apart from H, H_2 , C and C_2 that have no absorption in the mid-infrared region. Fig. 3 shows partial difference spectra of isotopic samples for solid methane after photolysis at 121.6 nm for 76 min. These difference spectra were derived on subtracting the spectra recorded after irradiation from the spectra before irradiation; in these spectra, lines pointing upwards indicate production, whereas those pointing downwards indicate destruction. After photolysis, many new features appeared, shown in Fig. 3; the wavenumbers of these lines and their assignments appear in Table 3.

We identified three stable products – C_2H_2 , C_2H_4 , C_2H_6 – and CH_3 radicals, in their various isotopic species, upon photolysis of pure solid methane at 121.6 nm based on our survey data as mentioned above. Irradiation of pure solid $^{12}\text{CH}_4$ produced characteristic lines of $^{12}\text{C}_2\text{H}_2$ at 736.6 (ν_5) and 3267.4 cm^{-1} (ν_3), of $^{12}\text{C}_2\text{H}_4$ at 949.7 (ν_7) and 1437.3 cm^{-1} (ν_{12}), and of $^{12}\text{C}_2\text{H}_6$ at 820.3 (ν_{12}), 1373.3 (ν_6), 1463.9 (ν_{11}), 2883.9 (ν_5), 2942.0 (ν_1) and 2976.1 cm^{-1} (ν_{10}). A line at 609.0 cm^{-1} after irradiation of pure solid $^{12}\text{CH}_4$ is characteristic of $^{12}\text{CH}_3$ radicals, vibrational mode ν_2 , but of no other likely compound or identifiable species, and is confirmed by both a shift to 604.1 cm^{-1} for $^{13}\text{CH}_3$ after analogous photolysis of $^{13}\text{CH}_4$ and the result of quantum-chemical calculations

Table 2. Calculated A-factors/ km mol^{-1} and experimental values of characteristic absorption lines of CH_3 , C_2H_4 , C_2H_6 and C_2H_2 .

Species	Mode	ν/cm^{-1}	Theory		Experiment	
			A-factor	Ratio	Area/ cm^{-1}	Ratio
CH_3	ν_2	609.0	73.9	37.7	–	–
C_2H_2	ν_5	736.6	196	100.0	0.0785 ± 8.3 per cent	100 ± 8.3
C_2H_4	ν_7	949.7	97.1	49.5	0.0441 ± 8.7 per cent	56.2 ± 8.7
C_2H_6	ν_{10}	2975.7	129	65.7	0.0569 ± 3.5 per cent	72.5 ± 3.5

Table 3. Products of photolysis at 121.6 nm of pure solid isotopic methanes at 3 K and their absorption lines.

$^{12}\text{CH}_4$		$^{13}\text{CH}_4$		$^{12}\text{CD}_4$	
Species	Wavenumber/cm $^{-1}$	Species	Wavenumber/cm $^{-1}$	Species	Wavenumber/cm $^{-1}$
$^{12}\text{CH}_3$	609.0 (ν_2)	$^{13}\text{CH}_3$	604.1 (ν_2)	$^{12}\text{CD}_3$	–
$^{12}\text{C}_2\text{H}_2$	736.6 (ν_5), 3267.4 (ν_3)	$^{13}\text{C}_2\text{H}_2$	734.5 (ν_5)	$^{12}\text{C}_2\text{D}_2$	2425.5 (ν_3)
$^{12}\text{C}_2\text{H}_4$	949.7 (ν_7), 1437.3 (ν_{12})	$^{13}\text{C}_2\text{H}_4$	944.8 (ν_7), 1431.1 (ν_{12})	$^{12}\text{C}_2\text{D}_4$	721.5 (ν_7), 1055.1 (ν_{12}), 2215.8 (ν_{11})
$^{12}\text{C}_2\text{H}_6$	820.3 (ν_{12}), 1373.3 (ν_6), 1463.9 (ν_{11}), 2883.9 (ν_5), 2942.0 (ν_1), 2976.1 (ν_{10})	$^{13}\text{C}_2\text{H}_6$	819.9 (ν_{12}), 1364.5 (ν_6), 1460.2 (ν_{11}), 2879.5 (ν_5), 2939.4 (ν_1), 2966.3 (ν_{10})	$^{12}\text{C}_2\text{D}_6$	593.8 (ν_{12}), 1069.1 (ν_{11}), 2079.9 (ν_5), 2129.6 (ν_1), 2230.8 (ν_{10})
U ^a	2958.5			U ^a	712.6

Note. ^aUnidentified line.

(Gaussian 09, MP2/aug-cc-pvqz). For $^{12}\text{CD}_3$, ν_2 shifts to about 460 cm^{-1} beyond our range of detection. A summary of wavenumbers of absorption lines and assignments, including isotopic variants, appears in Table 3.

3.4 Temporal profiles of photolysis at 121.6 nm

To assess the temporal depletion of precursor methane and the formation of the varied photolysis products, we photolyzed the methane samples for periods 10 s, 30 s, 1 min, 5 min, 10 min, 30 min and another 30 min sequentially; the total duration of irradiation is accordingly 76 min and 40 s. The temporal profiles of the depletion ratio for CH_4 and of formation for CH_3 , C_2H_2 , C_2H_4 and C_2H_6 upon photolysis at 121.6 nm are displayed in Fig. 4. As the integrated photon flux from our synchrotron is constant over time, the photon

dose is linearly proportional to the duration of exposure to the light from the synchrotron.

The depletion of methane amounted to about 24 per cent at 121.6 nm after 76 min, as shown in Fig. 4(a); although it is almost linear in the initial period of photolysis, it became non-linear after about 2 min. Little further depletion of methane occurred after 46 min. Fig. 4(b) displays temporal profiles of the formation of photolysis products CH_3 , C_2H_2 , C_2H_4 and C_2H_6 at 121.6 nm. The temporal profile of relative yield for the formation of CH_3 increased in the initial 2 min and decreased a little afterwards. The yields of C_2H_2 and C_2H_4 increased rapidly in the initial irradiation periods up to 10 min and approached plateau values. For C_2H_6 , the yield increased smoothly to 46 min and decreased afterwards.

These temporal profiles of formation for photoproducts indicate that photochemically initiated secondary reactions occurred under the conditions of our experiments. According to Fig. 4, the depletion of methane and the formation of products remained nearly constant after 76 min. This result might indicate that the depletion of methane and the abundance of photolysis products were near that of a steady state after irradiation for 76 min.

3.5 Photolysis products versus wavelength

The wavelength of light to which solid methane is exposed might affect the nature or proportions of the products of photolysis. To test this possibility, we subjected samples of pure solid CH_4 to photolysis at wavelengths 130, 140, 155, 165, 175, 185, 190 and 200 nm. Fig. 5 shows partial difference absorption spectra of pure solid methane irradiated at these wavelengths; the absorption lines of CH_3 , C_2H_2 , C_2H_4 and C_2H_6 are marked to clarify these photolysis products.

Upon examination of the spectra in Fig. 5, we found that the same four products – CH_3 , C_2H_2 , C_2H_4 and C_2H_6 – were produced upon photolysis at 130 nm as at 121.6 nm. The temporal depletion of methane and the temporal profiles of photolysis products at 130 nm (see supplementary information) are similar to those at 121.6 nm. The products and their proportions altered at wavelengths greater than 130 nm. After irradiation at 140 nm, the signal of C_2H_6 remained, but the signals of C_2H_2 and C_2H_4 decreased substantially and of CH_3 persisted with minute intensity. Upon photolysis at 155 and 165 nm, we detected no CH_3 and C_2H_4 , but the relative intensity of C_2H_2 increased to become comparable with that of C_2H_6 . Upon excitation at 175 nm, both C_2H_2 and C_2H_6 survived, but only a weak signal of C_2H_2 lingered upon irradiation at 185 and 190 nm. No product was observed after irradiation at 200 nm. The largest wavelengths at which products CH_3 , C_2H_4 , C_2H_6 and C_2H_2 of

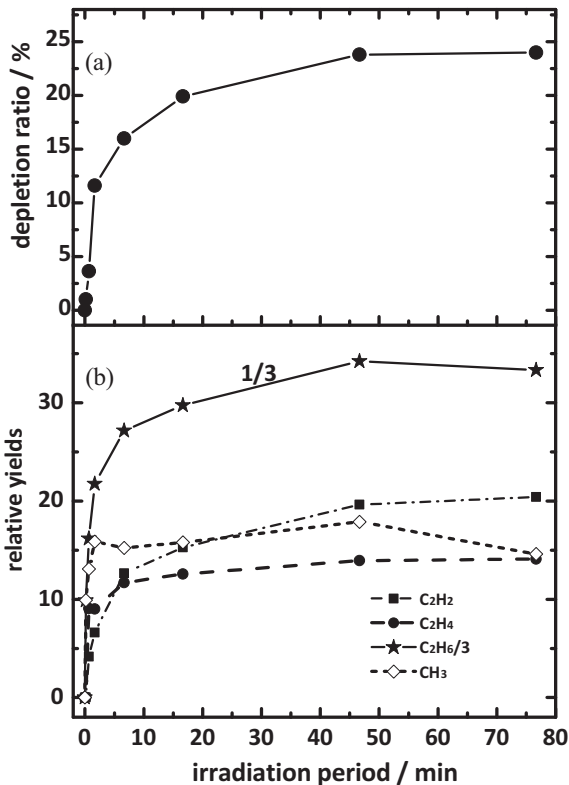


Figure 4. For pure CH_4 at 3 K irradiated at 121.6 nm; (a) temporal profile of depletion ratio for CH_4 ; (b) temporal profiles of the formation of CH_3 , C_2H_2 , C_2H_4 and C_2H_6 . The relative yield of C_2H_6 is divided by 3.

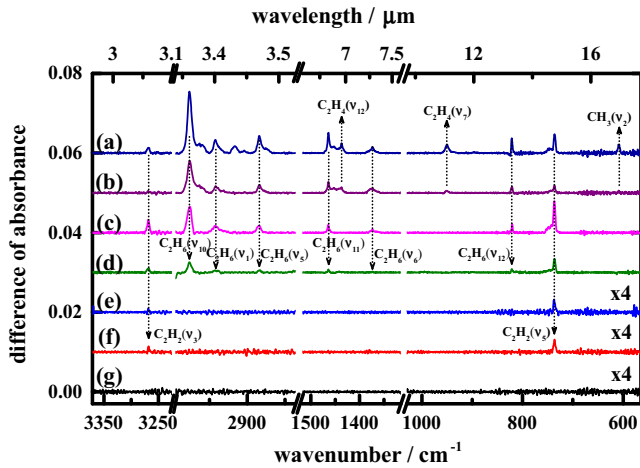


Figure 5. Difference spectra of solid methane after irradiation at 3 K at wavelengths (a) 130, (b) 140, (c) 165, (d) 175, (e) 185, (f) 190 and (g) 200 nm; the curves of (e), (f) and (g) are enlarged four times.

photolysis of solid methane were detected were 140, 140, 175 and 190 nm, respectively.

Based on the ratios of characteristic absorptions for various products, we derived the relative yields of these products at various wavelengths. According to the survey experiments, the ratios of absorptions $A(\text{C}_2\text{H}_2, \nu_5) : A(\text{C}_2\text{H}_4, \nu_7) : A(\text{C}_2\text{H}_6, \nu_{10})$ are 100 : 56.2 : 72.5, as listed in Table 2. For the absorption of CH_3 , a direct calibration for CH_3 is impracticable from a survey experiment as mentioned above; we instead estimated its relative value for mode ν_2 using calculated A-factor 73.9 km mol^{-1} and derived the ratio to be 37.7, also listed in Table 2. Among the photolysis products, C_2H_2 was detected at the greatest wavelength; we adopted its absorption at 736.6 cm^{-1} as 100 upon photolysis of CH_4 at 165 nm for comparison. Although our quantities of methane deposited were the same in all experiments, the photon doses at various wavelengths were not kept constant. We hence could not directly derive the relative yields of photolysis products at various wavelengths, but only their relative abundances, as listed in Table 4.

3.6 Comparison with the photochemistry of methane dispersed in neon

The efficiency of photolysis of methane and the nature of the products depended on the wavelength selected for irradiation. Our photolysis of pure solid methane at 121.6 nm at 3 K generated four identifiable products – CH_3 , C_2H_2 , C_2H_4 and C_2H_6 – that we identified according to their characteristic infrared absorption lines. In

contrast, our preceding experiments (Lin et al. 2014) on photolysis at 121.6 nm of methane dispersed in solid neon at 3 K, at ratios 1:100 to 1:10 000, yielded many more products, comprising CH_3 , C_2H_2 , C_2H_3 , C_2H_4 , C_2H_6 , C_4H_2 , C_4H_4 , C_5H_2 and C_8H_2 , C_nH ($n = 1-5$), and carbon chains C_n ($n = 3-20$); not only the production but also the yield of carbon agglomerates increased with a decreasing initial concentration of methane dispersed in solid neon. For example, at $\text{CH}_4:\text{Ne} = 1:100$, the products with 121.6 nm were stable molecules C_2H_2 , C_2H_4 , C_2H_6 , C_4H_2 and radicals CH_3 , C_2H_3 , C_3H , C_4H , C_5H , C_6 , whereas at $\text{CH}_4:\text{Ne} = 1:10\,000$, the 30 products included stable molecules C_2H_2 , C_2H_4 , C_2H_6 , C_4H_2 , C_4H_4 , oxides CO and C_5O , hydride radicals CH , CH_3 , C_2H_3 , C_2H , C_3H , C_4H , C_5H , C_5H_2 , C_8H_2 , and carbon chains C_3 , C_4 , C_5 , C_6 , C_7 , C_8 , C_9 , C_{10} , C_{11} , C_{12} , C_{14} , C_{16} , C_{18} and C_{20} (Lin et al. 2014). The photolysis of methane in a solid sample is thus affected to a large extent by the environment of the methane molecules.

The comparison with the photochemistry of methane dispersed in neon exposes another disparity regarding a dissociation threshold. No product of photolysis of methane was detectable on irradiation of methane dispersed in neon at wavelength larger than 150 nm, whereas methane was photolyzed to produce C_2H_2 at 190 nm in a pure solid state. A novel finding in our present work is that the largest wavelengths at which products C_2H_6 , C_2H_4 and C_2H_2 were generated were 175, 140 and 190 nm, respectively, through a radiative process: the greatest molecular disruption occurred with the photons of least energy.

3.7 Mechanism of photochemical decomposition of pure solid methane

The standard enthalpies of reaction at 300 K and the corresponding thresholds of wavelength for the dissociation of gaseous methane into other atomic and molecular species in their ground electronic states, plus excited methylene, are listed in Table 5.

According to Table 5, CH_4 might therefore dissociate at wavelengths greater than 110 nm according to equations (1a)~(1e) and (1g). The most abundant product of photolysis of gaseous methane at 121.6 or 118.2 nm is the CH_2 radical in its excited singlet state, a , whereas only a small fraction of CH_2 is formed in its ground triplet state, X (Gans et al. 2011). In the solid state, all six channels might hence be open. In our experiments, CH_4 might thus be photolyzed via equations (1a)~(1e) and (1g) at 121.6 and 130 nm, via equations (1a), (1b), (1c) and (1g) at 140 nm, and via equations (1a), (1b) and (1c) at wavelengths greater than 152 nm.

In pure solid methane, primary photolysis products C , CH and CH_2 are not detected; as they are generated with extra energy upon excitation with far-UV light, these species are highly reactive and

Table 4. Relative abundances of products of photolysis of CH_4 for 76 min at various wavelengths, relative photon doses (RPD) and depletion of CH_4 .

λ/nm	121.6	130	140	155	165	175	185	190	200
RPD ^a	39.0	246	169	36.6	100	72.0	59.1	38.9	29.6
$D(\text{CH}_4)^b$	24	35	4.8	2	6	< 0.5	< 0.5	< 0.5	0
CH_3	113	20.9	< 0.8	0	0	0	0	0	0
C_2H_2	158	25.6	14.0	42.6	100	60.5	11.6	18.6	0
C_2H_4	109	30.2	6.2	0	0	0	0	0	0
C_2H_6	775	130	112	113	123	56.6	0	0	0

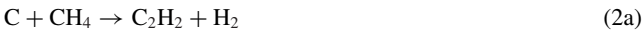
Notes. ^aRelative photon dose: total dose at 165 nm is 4.45×10^{18} photons, taken as 100.

^b $D(\text{CH}_4)$ = depletion ratio of CH_4 in %.

Table 5. Standard enthalpies of reaction at 300 K and the corresponding thresholds of wavelength for the dissociation of gaseous methane into other atomic and molecular species in their ground states, except CH₂ also in excited state.

	$\Delta_r H^\circ / \text{kJ mol}^{-1}$	$\lambda_{\text{threshold}} / \text{nm}$	
CH ₄ + $h\nu$ → CH ₃ + H	442	270.5	(1a)
→ CH ₂ X + H ₂	466.5	256.4	(1b)
→ CH ₂ <i>a</i> + H ₂	518.6	230.7	(1c)
→ CH ₂ X + 2H	902.5	132.5	(1d)
→ CH + H + H ₂	887	134.8	(1e)
→ CH + 3H	1323	90.4	(1f)
→ C + 2H ₂	791.5	151.1	(1g)
→ C + 4H	1664	71.9	(1h)

might react with a CH₄ molecule to form molecules C₂H₂, C₂H₄ and C₂H₆ as follows:



In contrast, as we detected CH₃ directly, its reactivity with CH₄ might be less than CH and CH₂. We recorded the absorption of CH₃ at wavelengths 121.6, 130 and 140 nm, but not at 155, 165, 175, 185, 190 and 200 nm in this work. This result is consistent with our previous work, in which the absorption of CH₃ was observed from CH₄ dispersed in solid neon at wavelengths 121.6, 130 and 140 nm, but not at wavelength greater than 150 nm (Lin et al. 2014). Including this work, the largest wavelength to form CH₃ from solid methane is 140 nm and corresponding energy is 8.57 eV, which is 4.27 eV greater than its minimum dissociation energy of 4.58 eV (270.5 nm) in the gaseous phase. In the solid state, impeded by the surrounding CH₄ molecules, CH₃ as a fragment might be constrained typically to remain at or near its site of origin, and to recombine with an H atom, unless either fragment has sufficient kinetic energy to escape to become isolated separately. On photodissociation of solid methane at a wavelength beyond 140 nm, isolated CH₃ might thus not be formed, whereas the formation of CH₃ at wavelengths less than 140 nm produces some energetic CH₃ radicals with extra energy, even above 4 eV; as result, these energetic CH₃ might react with CH₄ as follows:



As the region of ultraviolet absorption of C₂H₆ is similar to that of CH₄ but with a range slightly extended to greater wavelength, C₂H₄ also absorbs strongly at wavelengths less than 210 nm, their secondary photolysis reactions are likely important. Secondary photolysis of reaction products C₂H₆ and C₂H₄ can occur in the solid state, to generate C₂H₄ and C₂H₂, respectively.



Reactions (1)–(7) hence account for the four identified products – CH₃, C₂H₂, C₂H₄ and C₂H₆ – produced on irradiation of pure solid methane at 121.6, 130 and 140 nm.

For wavelengths greater than 154 nm, photolysis of methane can produce radicals CH₂ through reaction channels (1b) and (1c) (Bach et al. 1993). Primary photoproduct CH₂ might subsequently react with an adjacent CH₄ molecule in the solid state to generate C₂H₆, C₂H₄ and C₂H₂ via reaction (4) depending on its energy; during the photolysis, the generated CH₂ possesses atypical extra energy from upon different wavelength. As we observed C₂H₂ and C₂H₆ at 155, 165 and 175 nm, and only C₂H₂ at 185 and 190 nm, reaction (4b) does not seem to occur to form C₂H₄ for a wavelength larger than 154 nm; reaction (4a) appears not to produce C₂H₆ for wavelengths larger than 175 nm.

After photolysis of solid methane at 185 or 190 nm, the appearance of absorption lines at 736.6 and 3267.4 cm⁻¹ with intensities in the observed proportion, as are clear in Fig. 5, serves as an absolutely unambiguous signature for the production of C₂H₂. The signals of C₂H₂ are weak, resulting from less than 0.5 per cent depletion of precursor CH₄. According to the first law of photochemistry, the appearance of detectable products on exposure of methane samples to light at 185 or 190 nm is proof of the absorption by the sample at those wavenumbers, even though that absorption is undoubtedly weak. The possibility of the photolysis being caused by stray light of appreciably smaller wavelength is completely excluded because of the quartz filter that was applied for photolysis at 185 and 190 nm; in any case, such stray light would have generated detectable products other than C₂H₂, according to our own definitive observations. The temporal profile of the formation of C₂H₂ represented by the integrated area of absorption line at 736.6 cm⁻¹ upon photolysis of pure solid CH₄ at 190 nm is displayed in Fig. S2 (see supplementary information); the weak signals of C₂H₂ appear to increase steadily with time up to 76 min. On detailed examination, the temporal profiles of the formation of C₂H₂ at 185 and 190 nm (Fig. S2, supplementary information) differ from those at 121.6 (Fig. 4) and 130 nm (Fig. S1, supplementary information); this phenomenon might indicate that the mechanism of the formation of C₂H₂ at 185 and 190 nm differs from that at other and smaller wavelengths. Reactions (2), (3), (4), (5) and (7) might be inapplicable for a photolysis wavelength greater than 175 nm.

The formation of C₂H₂ is mysterious, especially for photolysis wavelength greater than 175 nm; Milligan & Jacox (1967) recorded infrared absorption spectra of not only CH₃ but also C₂H₂ on photolysis, at 121.6 nm, of CH₄ dispersed in solid argon at 14 K, under conditions in which secondary photolysis and secondary reactions were likely negligible, but these authors offered no explanation of the latter observation. For the formation of C₂H₂, one plausible reaction is from the self-reaction of CH₂:



As another possibility in solid methane upon photolysis, if two adjacent or near CH₄ molecules produce two CH₂ through separate excitation by photons, these two CH₂ could react and produce C₂H₂. The energy of two energetic CH₂ radicals is large in the self-reaction system. Due to the lack of a way to release the excess energy, this self-reaction might not form stabilized adduct C₂H₄ in the reaction system; dissipating the excess energy through product H₂, reaction (8) can thus proceed. This reaction can occur at all wavelengths to

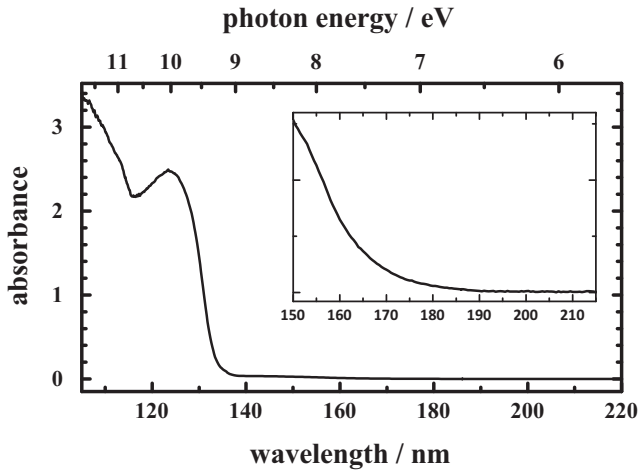


Figure 6. VUV absorption spectrum of pure solid CH₄ at 10 K in the spectral region 106–220 nm at resolution 0.2 nm. The inset displays the enlarged scale beyond 150 nm.

a minor extent, but it can become dominant when, according to the lack of their products, reactions (2)–(7) do not occur at 185 and 190 nm.

3.8 Photochemical decomposition of methane clusters

From our previous works, the far-UV absorption of gaseous methane possesses an apparent onset about 145 nm (8.55 eV), whereas the value of methane dispersed in neon shifts to about 150 nm (Lin et al. 2014). Fig. 6 displays absorption spectrum of pure solid CH₄ at 10 K in the spectral region 106–220 nm at resolution 0.2 nm. The far-UV absorption of pure solid methane extends to 190 nm; this indicates that the absorption beyond 150 nm is associated with the methane clusters.

For wavelengths larger than 150 nm, irradiation of sample CH₄/Ne (1/1000) produces no photoproduct (Lin et al. 2014); an isolated CH₄ molecule (or CH₄ monomer) in solid neon is hence inert at wavelengths greater than 150 nm. However, we observed C₂H₂ and C₂H₆ from pure solid methane upon irradiation at wavelengths larger than 150 nm; this effect indicates that at these wavelengths products C₂H₂ and C₂H₆ might be formed not from the CH₄ monomer, but from a cluster. As mentioned above, the infrared absorption spectra of methane reveal a significant intermolecular interaction in the pure solid state; this interaction yields infrared absorption of pure solid CH₄ extended to broad lines, as shown in Fig. 1. For example, the ν_4 band of pure solid CH₄ exhibits a partially resolved doublet at 1301.5 and 1296.8 cm⁻¹ with a shoulder at 1294.5 cm⁻¹; this doublet possesses a total width about 8.2 cm⁻¹. Such a width reflects the interaction between molecules, two or more at a time, in the lattice.

After irradiation with far-UV light, the difference absorption spectra show patterns depending on the excitation wavelength. For example, Fig. 7 displays two typical difference IR absorption spectra of solid methane at 3 K after irradiation at wavelengths 121.6 and 185 nm in the region 1270–1320 cm⁻¹. Upon excitation at 121.6, 130 and 140 nm, the spectra are similar in Fig. 7(b), which develops three downward lines at about 1302, 1297 and 1294 cm⁻¹. In contrast, Fig. 7(a) shows two upward lines about 1302 and 1297 cm⁻¹ and one downward line at 1294 cm⁻¹; upon irradiation with light of wavelength greater than 150 nm, the spectra possess the same pattern as this curve. The downward line in the difference ab-

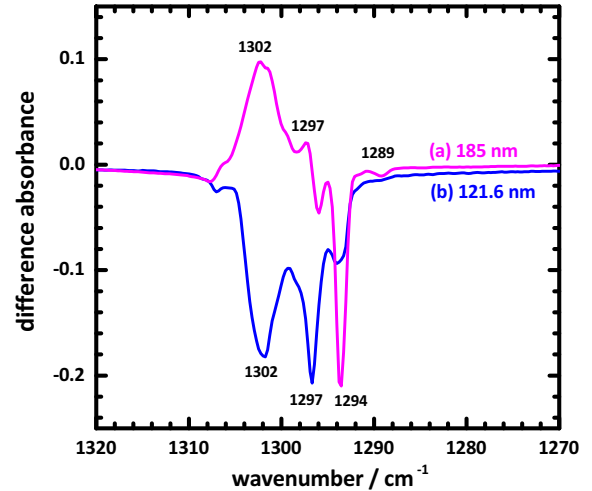


Figure 7. Difference of IR absorption spectra of solid methane at 3 K after irradiation with wavelengths (a) 185 and (b) 121.6 nm in the region 1270–1320 cm⁻¹.

sorption spectra means depletion of the absorption line. The species associated with downward lines 1302, 1297 and 1294 cm⁻¹ were all depleted at 121.6, 130 and 140 nm. As mentioned above, the CH₄ monomer is not susceptible to photolysis for wavelengths beyond 150 nm; the depletion line at 1294 cm⁻¹ in Fig. 7(a) is associated not with a single CH₄ molecule but with some aggregate, likely a CH₄ dimer constituting two methane molecules in close proximity. Such a CH₄ dimer can certainly be dissociated in the far-UV region; its photolysis would yield products involving either two methane molecules in less close proximity or less interacting, or molecules containing two carbon atoms, as observed. The former process results in regenerated CH₄ monomer and decreased CH₄ dimer. Accordingly, the upward lines 1302 and 1297 cm⁻¹ might be contributed by the CH₄ monomer, whereas the downward line 1294 cm⁻¹ belongs to the CH₄ dimer.

On irradiation of solid methane with light of wavelength greater than 150 nm, all difference absorption spectra contain the depletion line 1294 cm⁻¹ that might be attributed to the CH₄ dimer. This result indicates that methane clusters, such as a dimer, might play an important role in the photochemistry of pure solid methane at these wavelengths. As photolysis products C₂H₂ and C₂H₆ containing two carbon atoms are reasonably formed via a radiatively induced reaction of adjacent molecules in the pure solid state, we expect that C₂H₂ and C₂H₆ might be formed via a reaction initiated within a methane dimer at the pertinent wavelengths:



Any mechanism of any reaction is purely speculative, including that above. We emphasize that the highly effective filters that we employ in these experiments absolutely preclude the indicated photochemical processes as a result of stray light of smaller wavelength. Under these conditions, a mechanism involving the photolysis of interacting molecules in solid methane, likely two at a time, becomes plausible.

3.9 Implications for photochemistry in space

Methane is observed in space objects at concentrations such as 1.6 per cent on Titan (Hirtzig et al. 2009), 4.7 per cent for young

stellar objects (Öberg et al. 2008) and 0.2~1.45 per cent for comets (Brooke et al. 2003; Magee-Sauer et al. 2008). Like water clouds on Earth, methane may exist as clouds in these astronomical objects; the cycling of methane clouds subsequently condenses methane into lakes or oceans in astronomical environments, similar to water on Earth. Radar images from spacecraft *Cassini* on Titan indicated more than 75 radar-dark patches that are attributed to lakes of liquid methane (Stofan et al. 2007); this evidence demonstrates the existence of pure condensed methane in astro-environments. Consistent with the melting point of methane about 90 K, methane is known to exist in a solid form in outer space at less than 40 K (Quirico et al. 1999; Olkin et al. 2007; Tegler et al. 2010). Our photochemical experiments on pure solid methane are thus applicable to astronomical environments. Shemansky et al. reported that the number densities of CH₄, C₂H₂, C₂H₄ and C₂H₆ are 1.90×10^{17} , 1.11×10^{16} , 8.2×10^{15} and 7.3×10^{15} molecules per mL, respectively, on Titan (Shemansky et al. 2005). In this work, we observed stable molecules C₂H₂, C₂H₄ and C₂H₆ upon excitation at 121.6, 130 and 140 nm, C₂H₂ and C₂H₆ at 155, 165 and 175 nm, and only C₂H₂ at 185 and 190 nm; our results might be linked to this observation.

4 CONCLUSION

With light of wavelength 120–200 nm selected from a synchrotron source, we irradiated samples of pure solid methane at 3 K. After irradiation, four distinct products – CH₃, C₂H₂, C₂H₄ and C₂H₆ – were identified according to their characteristic infrared absorption lines. The distribution among these products depended on the wavelength of irradiation. We observed all four products upon excitation at 121.6, 130 and 140 nm, C₂H₂ and C₂H₆ at 155, 165 and 175 nm, and only C₂H₂ at 185 and 190 nm. No product was observed after irradiation at 200 nm. The largest wavelengths at which products CH₃, C₂H₄, C₂H₆ and C₂H₂ were detected were 140, 140, 175 and 190 nm, respectively. We compare our result with previous work (Lin et al. 2014) on irradiation of methane dispersed in solid Ne at 3 K. Information about the dissociation of CH₄ at low temperature with photons of varied energy has implications for astrophysical environments.

ACKNOWLEDGEMENTS

National Science Council of Taiwan (grant NSC 102-2113-M-213-005-MY3) and NSRRC provided support for this research.

REFERENCES

- Alexander R. D., Casali M. M., André P., Persi P., Eiroa C., 2003, *A&A*, 401, 613
 Bach R. D., Su M. D., Aldabbagh E., Andres J. L., Schlegel H. B., 1993, *J. Am. Chem. Soc.*, 115, 10237
 Baratta G., Domingo M., Ferini G., Leto G., Palumbo M., Satorre M., Strazzulla G., 2003, *Nucl. Instrum. Methods Phys. Res. B*, 209, 283
 Bennett C. J., Jamieson C. S., Osamura Y., Kaiser R. I., 2006, *ApJ*, 653, 792
 Brooke T. Y., Weaver H. A., Chin G., Bockelée-Morvan D., Kim S. J., Xu L.-H., 2003, *Icarus*, 166, 167
 Cecchi-Pestellini C., Aiello S., 1992, *MNRAS*, 258, 125
 Chiar J. E., Tielens A. G. G. M., Whittet D. C. B., Schutte W. A., Boogert A. C. A., Lutz D., van Dishoeck E. F., Bernstein M. P., 2000, *ApJ*, 537, 749
 Cook P. A., Ashfold M. N. R., Jee Y.-J., Jung K.-H., Harich S., Yang X., 2001, *Phys. Chem. Chem. Phys.*, 3, 1848
 de Barros A. L. F., Bordalo V., Seperuelo Duarte E., da Silveira E. F., Domaracka A., Rothard H., Boduch P., 2011, *A&A*, 531, A160

- Dobbs K. D., Dixon D. A., 1994, *J. Phys. Chem.*, 98, 4498
 Frisch M. J. et al., 2009, *Gaussian 09 A02*. Gaussian, Inc., Wallingford CT
 Gans B. et al., 2011, *Phys. Chem. Chem. Phys.*, 13, 8140
 Gerakines P. A., Schutte W. A., Ehrenfreund P., 1996, *A&A*, 312, 289
 Gürtler J., Klaas U., Henning T., Ábrahám P., Lemke D., Schreyer K., Lehmann K., 2002, *A&A*, 390, 1075
 Hirtzig M., Tokano T., Rodriguez S., Mouélic S. le, Sotin C., 2009, *A&AR*, 17, 105
 Jamieson C. S., Bennett C. J., Mebel A. M., Kaiser R. I., 2005, *ApJ*, 624, 436
 Kaiser R. I., Roessler K., 1998, *ApJ*, 503, 959
 Lin M.-Y., Lo J.-I., Lu H.-C., Chou S.-L., Peng Y.-C., Cheng B.-M., Ogilvie J. F., 2014, *J. Phys. Chem. A*, 118, 3438
 Magee-Sauer K., Mumma M. J., DiSanti M. A., Dello Russo N., Gibb E. L., Bonev B. P., Villanueva G. L., 2008, *Icarus*, 194, 347
 Markwick A. J., Millar T. J., Charnley S. B., 2000, *ApJ*, 535, 256
 Milligan D. E., Jacox M. E., 1967, *J. Chem. Phys.*, 47, 5146
 Mount G. H., Rottman G. J., 1983, *J. Geophys. Res.*, 88, 5403
 Öberg K. I., Boogert A. C., Pontoppidan K. M., Blake G. A., Evans N. J., Lahuis F., van Dishoeck E. F., 2008, *ApJ*, 678, 1032
 Ogilvie J. F., Chou S.-L., Lin M.-Y., Cheng B.-M., 2011, *Vib. Spectrosc.*, 57, 196
 Olkin C. B. et al., 2007, *AJ*, 133, 420
 Quirico E., Douté S., Schmitt B., de Bergh C., Cruikshank D. P., Owen T. C., Geballe T. R., Roush T. L., 1999, *Icarus*, 139, 159
 Romanzin C. et al., 2005, *Adv. Space Res.*, 36, 258
 Rottman G. J., 1981, *J. Geophys. Res.*, 86, 6697
 Shemansky D. E., Stewart A. I. F., West R. A., Esposito L. W., Hallett J. T., Liu X., 2005, *Science*, 308, 978
 Spoon H. W. W., Keane J. V., Tielens A. G. G. M., Lutz D., Moorwood A. F. M., 2001, *A&A*, 365, L353
 Stofan E. R. et al., 2007, *Nature*, 445, 61
 Tegler S. C. et al., 2010, *ApJ*, 725, 1296
 Wang J.-H., Liu K., 1998, *J. Chem. Phys.*, 109, 7105
 White G. J. et al., 2000, *A&A*, 364, 741
 Wu Y.-J., Lin M.-Y., Cheng B.-M., Chen H.-F., Lee Y.-P., 2008, *J. Chem. Phys.*, 128, 204509
 Wu Y.-J., Lin M.-Y., Chou S.-L., Chen H.-F., Lu H.-C., Chen H.-K., Cheng B.-M., 2010, *ApJ*, 721, 856
 Wu Y.-J., Wu C.-Y. R., Chou S.-L., Lin M.-Y., Lu H.-C., Lo J.-I., Cheng B.-M., 2012, *ApJ*, 746, 175
 Yung Y. L., DeMore W. B., 1999, *Photochemistry of Planetary Atmospheres*. Oxford University Press, New York

SUPPORTING INFORMATION

Additional Supporting Information may be found in the online version of this paper:

Figure S1. For pure CH₄ at 3 K irradiated at 130 nm, (a) temporal profile of depletion ratio for CH₄; (b) temporal profiles of formation of CH₃, C₂H₂, C₂H₄ and C₂H₆. The relative yield of C₂H₆ is divided by 3.

Figure S2. Temporal profile of formation of C₂H₂ represented by the integrated area of absorption line at 736.6 cm⁻¹ upon photolysis of pure solid CH₄ at 190 nm (<http://mnras.oxfordjournals.org/lookup/suppl/10.1093/mnras/stv935/-/DC1>).

Please note: Oxford University Press are not responsible for the content or functionality of any supporting materials supplied by the authors. Any queries (other than missing material) should be directed to the corresponding author for the paper.

This paper has been typeset from a $\text{\TeX}/\text{\LaTeX}$ file prepared by the author.